

1 **Unlinked Mendelian inheritance of red and black pigmentation in snakes: implications**
2 **for Batesian mimicry**

3 Alison R. Davis Rabosky^{1,2*}, Christian L. Cox³, and Daniel L. Rabosky¹

4 ¹Department of Ecology and Evolutionary Biology and Museum of Zoology, University of
5 Michigan, 1109 Geddes Ave., Ann Arbor, MI 48109, USA

6 ²Department of Integrative Biology and Museum of Vertebrate Zoology, University of
7 California, Berkeley, California 94720

8 ³Department of Biology, Georgia Southern University, PO Box 8042, Statesboro, GA, 30460,
9 USA

10 *corresponding author: ardr@umich.edu

11 A Brief Communication for *Evolution*

12

13 **Running head:** Genetics of mimetic coloration in snakes

14 **Keywords:** coral snake mimicry, coloration genetics, color polymorphism, supergene,
15 linkage disequilibrium, *Sonora semiannulata*

16 **Data archival:** Supplementary data files are included with this manuscript and archived at
17 Dryad (upon acceptance; *doi placeholder*)

This is the author manuscript accepted for publication and has undergone full peer review but has not been through the copyediting, typesetting, pagination and proofreading process, which may lead to differences between this version and the [Version of Record](#). Please cite this article as [doi: 10.1111/evo.12902](https://doi.org/10.1111/evo.12902).

This article is protected by copyright. All rights reserved.

18 **Abstract**

19 Identifying the genetic basis of mimetic signals is critical to understanding both the
20 origin and dynamics of mimicry over time. For species not amenable to large laboratory
21 breeding studies, widespread color polymorphism across natural populations offers a
22 powerful way to assess the relative likelihood of different genetic systems given observed
23 phenotypic frequencies. We classified color phenotype for 2,175 ground snakes (*Sonora*
24 *semiannulata*) across the continental United States to analyze morph ratios and test among
25 competing hypotheses about the genetic architecture underlying red and black coloration in
26 coral snake mimics. We found strong support for a two-locus model under simple Mendelian
27 inheritance, with red and black pigmentation being controlled by separate loci. We found no
28 evidence of either linkage disequilibrium between loci or sex linkage. In contrast to Batesian
29 mimicry systems like butterflies in which all color signal components are linked into a single
30 “supergene,” our results suggest that the mimetic signal in colubrid snakes can be disrupted
31 through simple recombination and that color evolution is likely to involve discrete gains and
32 losses of each signal component. Both outcomes are likely to contribute to the exponential
33 increase in rates of color evolution seen in snake mimicry systems over insect systems.

Author Manuscript

34 **Introduction**

35 Mimicry, in which two unrelated species converge upon a novel phenotype for the
36 purpose of signaling to predators, is a classic system for understanding the mechanisms that
37 drive transitions to strikingly new and distinct character states (Mallet and Joron 1999; Reed
38 et al. 2011). “Warning signals” in mimicry systems are usually complex traits composed of
39 multiple distinct elements that are all required for the signal to be effective, especially for
40 coloration (Mappes and Alatalo 1997; Kronforst and Papa 2015). Understanding the genetic
41 determinants of these warning signals is important because theoretical models predict that the
42 genomic architecture of signal components should vary across different kinds of mimicry
43 systems (Charlesworth and Charlesworth 1975; Turner 1987; Charlesworth 2016). In
44 Müllerian mimicry systems in which all members are toxic (or otherwise defended), no
45 genetic linkage is necessary between signal components to promote the evolution of the trait.
46 However, strong linkage into polymorphic “supergenes” is predicted for Batesian systems in
47 which some members are completely undefended (Charlesworth and Charlesworth 1975).
48 This difference in predictions is due to whether or not recombinant types that express just one
49 of the traits (*e.g.*, conspicuous, but not mimetic) suffer reduced fitness in the early evolution
50 of a multi-component mimetic phenotype, which theoretically should affect novel Batesian,
51 but not Müllerian, mimics. In the face of strong selection against undefended conspicuous
52 recombinants, linkage between the signal component loci should evolve rapidly
53 (Charlesworth and Charlesworth 2011).

54 For the mimicry systems in which we best understand the genetic architecture
55 underlying signal components (primarily coloration in butterflies), these predictions are fairly
56 well supported. There is strong evidence that mimetic loci are organized into polymorphic
57 supergenes in the Batesian *Papilio* (Kunte et al. 2014) and some *Heliconius* butterflies (Joron
58 et al. 2006; Joron et al. 2011) achieved through chromosomal rearrangement and inversions,

59 while the majority Müllerian *Heliconius* species retain critical coloration components on
60 separate chromosomes (Kronforst and Papa 2015). In both kinds of mimicry systems, the
61 predominant pattern is that there are a few loci of major effect with a number of smaller
62 modifier loci (Nijhout 2003; Franks and Sherratt 2007; Gamberale-Stille et al. 2012; Leimar
63 et al. 2012), and convergence among species on the same color phenotype is at least in some
64 cases driven by parallel evolution in the same genes (Reed et al. 2011; Martin et al. 2012).

65 Coral snake mimicry (the imitation of highly venomous Elapid coral snakes by
66 harmless Colubrid snakes across North and South America) offers an opportunity to
67 independently test the genetic predictions of Batesian mimicry systems. Although the
68 majority of coral snake mimics are not considered toxic to predators, the cost of
69 misidentifying an atypically colored coral snake would be very high (*i.e.*, death) relative to
70 the cost of misidentifying a noxious insect (Pough 1988). This critical difference in cost
71 could create altered fitness landscapes for recombinant types in the mimetic species. If
72 selection against misidentification is strong enough, then the “conspicuous recombinant” may
73 still be avoided by predators and linkage among signal components would not be generated.
74 As in butterfly mimics (Joron and Mallet 1998), many snake species involved in mimicry
75 systems have striking color polymorphism in the warning signal components (Savage and
76 Slowinski 1992; Davis Rabosky et al. in review). As polymorphism can arise through either
77 supergene or unlinked models of mimicry genes (Charlesworth 2016) but produces differing
78 frequencies of “recombinants,” this phenotypic variation can be leveraged to test among these
79 competing hypotheses about the genetic architecture underlying color expression (Wright
80 1943).

81 In coral snake mimicry, the warning coloration involves variations on highly
82 contrasting alternating bands, especially in black and red (Savage and Slowinski 1992;
83 Brodie and Brodie 2004). Color polymorphism within coral snake mimicry occurs through

84 variation in either of these two signal components, often by presence/absence to produce all
85 phenotypic combinations: 1) both red and black, 2) only red, 3) only black, and 4) neither
86 (Davis Rabosky et al. in review). Although comparatively little is known in snakes about the
87 genetic pathways driving synthesis and distribution of either pigment, they are thought to be
88 endogenously produced pteridines (likely drosopterins) and melanins, respectively (Bechtel
89 1978; Bagnara 1983; Kikuchi and Pfennig 2012; Kikuchi et al. 2014). The differing structural
90 morphology, biochemistry, and dermal layer distribution of the chromatophores that produce
91 each pigment (Kuriyama et al. 2013) in vertebrates suggest that red and black pigmentation
92 are likely controlled by separate genetic loci, which is bolstered by a limited set of common
93 garden breeding experiments using artificially selected color mutations in corn snakes
94 (Bechtel and Bechtel 1962, 1978). Although some quantitative genetic studies have found
95 correlation among pigment blotch sizes in garter snakes (Westphal and Morgan 2010;
96 Westphal et al. 2011), neither the genetic control nor linkage of red and black coloration has
97 ever been investigated within coral snake mimicry.

98 For organisms with long generation times and low reproductive output that are not
99 amenable to breeding studies within the laboratory, large-scale population sampling of color
100 polymorphism, in combination with the predictions of Hardy-Weinberg equilibrium, can
101 provide a powerful way to test among genetic models governing coloration in mimetic
102 species. In this study, we leveraged such population-level data in the polymorphic Western
103 Ground Snake (*Sonora semiannulata*) to test among a) one- vs. two-locus models, b) linkage
104 disequilibrium among loci, and c) sex-linked vs. autosomal models and assess the
105 relationship between observed and predicted genetic architecture of the mimetic signal in a
106 non-insect Batesian mimic.

107 **Materials and Methods**

108 *Study system*

109 The Western ground snake (*Sonora semiannulata*) is a small insectivorous snake
110 native to the western United States and northern Mexico. This species is best known for its
111 striking color polymorphism, with up to four discrete color morphs occurring sympatrically
112 within single populations (Cox and Davis Rabosky 2013). All four color morphs are found in
113 both sexes and all age classes, with no ontogenetic color change (Cox and Davis Rabosky
114 2013). These color morphs include all combinations of red and black pigmentation, including
115 individuals with a) both color components, b) only black, c) only red, and d) neither (Fig. 1).
116 The black and red morph of *S. semiannulata* is commonly interpreted as a mimic of
117 venomous coral snakes (Savage and Slowinski 1992; Brodie and Brodie 2004; Campbell and
118 Lamar 2004; Cox et al. 2012) due both to its striking similarity to coral snake color pattern
119 and to the evolutionary history of coloration within the larger tribe Sonorini, which also
120 suggests the origin and maintenance of the mimetic form in this clade for the last 25 million
121 years (Davis Rabosky et al. in review). Despite its importance in other squamates
122 (Rosenblum 2006; Rosenblum et al. 2010), we have found no link between the
123 melanogenesis gene *Mc1R* and black banding in Sonorine snakes (Cox et al. 2013).

124 *Population sampling and test for sex linkage*

125 To assess morph ratios within populations, we examined 2,175 fluid-preserved
126 specimens from the continental United States housed in 12 institutional collections (see
127 Acknowledgements). In addition to collecting specimen size (snout-vent length and tail
128 length) and sex data, we scored dorsal coloration on each specimen as mimetic red and black
129 (M), black-banded only (B), red-striped only (S), or a uniform brown or tan with neither type
130 of marking (U). Although some pigmentation fades in the preservation process, both stripes
131 and bands are readily visible against the remaining background body pigment even in 100-
132 year old museum specimens (Cox and Davis Rabosky 2013). Each snake was independently
133 scored by at least two researchers to ensure repeatability of phenotype scores.

134 To create a subset of individuals for population analysis of morph frequencies, we
135 filtered the overall dataset to populations with at least 12 individuals collected within a 20-
136 year window ($N = 40$ populations; see *Power analysis and simulations* below). For
137 populations with robust collection histories over long time periods, we used the single 20-
138 year window with the greatest number of specimens. We defined populations by county of
139 collection in order to maximize use of specimens without georeferenced latitude-longitude
140 coordinates. For each county, we recorded the number of specimens of each color morph, the
141 first year of the 20 year window used for that population, and the latitude and longitude for
142 the county midpoint using metrics from the U.S. Census Bureau (2011).

143 To assess whether coloration is sex-linked or autosomal, we conducted a chi-square
144 test against the expected number of males and females of each morph under a null
145 (autosomal) model to identify deviations suggesting sex linkage. First, we analyzed all
146 individuals for which we had reliable sex data ($N = 253$ females and 482 males), irrespective
147 of population. A greater proportion of males were sexable with high confidence because they
148 are sometimes preserved with the hemipenes everted, accounting for much of the difference
149 between the sexes in sample size. We also conducted within-population tests for every
150 population with a) at least 20 individuals overall, and b) at least 5 individuals of each sex, but
151 these analyses were limited by suitably-sized populations ($N = 7$).

152 *Tests for spatial and temporal autocorrelation*

153 To assess statistical independence of populations prior to analysis, we used Mantel
154 tests ($N = 999$ permutations) in the R package ‘vegan’ to test for both spatial and temporal
155 autocorrelation in morph frequencies. Because previous research found evidence that
156 negative frequency-dependent selection is operating to maintain polymorphism in at least
157 some populations (Cox and Davis Rabosky 2013), a temporal component was important to
158 include in our analyses. We calculated Euclidean distance matrices among populations based

159 on 1) both morph frequencies and morph presence/absence (two types of phenotypic
160 distance) and 2) time window start years (temporal distance), and by geodesic distance using
161 the Haversine formula after converting latitude/longitude coordinates to radians (geographic
162 distance). We then compared each phenotypic distance matrix with a) the geographic and
163 temporal distance matrices individually, as well as b) in combination within a partial Mantel
164 test framework. To mitigate the possibility of finding a spurious negative correlation across
165 both long distances and a known genetic clade break through central New Mexico (Davis
166 Rabosky et al. in review), we also repeated these analyses after dividing the overall dataset by
167 clade affiliation into “Western” and “Great Plains” clades (as in Table S1). Significance was
168 assessed at $P < 0.05$.

169 *Likelihood analysis of color morph genetics*

170 We defined three simple models for the inheritance of color phenotypes in ground
171 snakes: *one-locus*, *two-locus*, and *two-locus with linkage*. Under the one-locus model, we
172 assumed that color phenotype is a function of three alleles: red (r), black (b), and null (n). In
173 this model, the black and red alleles are co-dominant in the mimetic phenotype, and both are
174 dominant to the recessive null allele; this is the simplest genetic system that can lead to the
175 four observed morphs. For a given population, the likelihood of the data is simply the
176 probability of the observed phenotypic data given a vector of allele frequencies under the
177 assumption of Hardy-Weinberg equilibrium. For example, $2rb$ is the probability that a single
178 randomly sampled individual will show the mimetic phenotype, and $r^2 + 2rn$ is the
179 probability that an individual will exhibit the striped phenotype. The two-locus model
180 assumes that red and black pigmentation are coded by dominant alleles at separate,
181 independently-assorting loci. Each locus is assumed to have both a pigment-producing (r or
182 b) and null allele (n_r or n_b), and a snake that is homozygous for the null allele at both loci
183 would have uniform brown patterning. Note that for both models, the number of free

184 parameters per population is the same ($np = 2$), as allele frequencies for each locus must sum
185 to 1.

186 To test for linkage disequilibrium among loci, we added an additional parameter D to
187 the two-locus model that specified the extent of gametic disequilibrium for red and black
188 alleles. D is a purely statistical measure of the gametic association of alleles from different
189 loci. Letting n_r and n_b denote null alleles at the red and black loci, the gametic frequencies
190 are:

$$\begin{aligned}f(r, b) &= rb + D \\f(r, n_b) &= rn_b - D \\f(n_r, b) &= n_r b - D \\f(n_r, n_b) &= n_r n_b + D\end{aligned}$$

192 With $D = 0$, all gametic frequencies follow their expectation under independent assortment. D
193 > 0 implies an excess of rb gametes. D takes a maximum value that depends on the allele
194 frequencies. With $D > 0$, $D_{max} = \min(rn_b, n_r b)$: the maximum is necessary because, were D to
195 exceed this value, some gametic frequencies would be negative. The full probability model
196 for the phenotypic data is derived from the above frequencies. For example, the probability of
197 observing a mimetic phenotype is

$$198 \quad f(r, b)^2 + 2f(r, b)f(r, n_b) + 2f(r, b)f(n_r, b) + 2f(r, b)f(n_r, n_b) + 2f(n_r, b)f(r, n_b)$$

199 which is simply the sum of all genotypic frequencies that could yield a mimetic phenotype
200 under the model. We defined two versions of the two-locus model with linkage. In the first,
201 we treated D as a free parameter to be estimated separately for each population. For the
202 second model, we assessed the likelihood of the phenotypic data under *strong linkage*
203 between red and black alleles, as predicted by genetic models of mimicry. For this latter
204 model, we fixed the relative value of D ($D_{rel} = D / D_{max}$) to 0.99. This model assumes that the
205 red and black alleles will show gametic associations close to their theoretical maximum
206 value. Importantly, with a fixed relative D , the number of parameters per population is

207 identical to the two-locus model without linkage ($D = 0$).

208 The probability the data (X) is simply the product of the probabilities of observing
209 individual phenotypes across all K populations under the model (M) and parameters, or

$$210 \quad \Pr(X | M) = \prod_{k=1}^K \prod_{i=1}^{n_k} \Pr(x_{i,k} | M, \theta_k)$$

211 where n_k is the number of individuals in the k 'th population, $x_{i,k}$ is the observed phenotype for
212 the i 'th individuals from population k , and θ_k is the parameter vector for the k 'th population.

213 We implemented all inheritance models in the R programming language (Dryad doi:
214 *placeholder*), finding maximum likelihood estimates of parameters using a Nelder-Mead
215 simplex algorithm on a logit-transformed parameter space. We fitted all models to the
216 observed phenotype counts for each population, estimating allele frequencies and linkage
217 parameters (if relevant).

218 We computed ΔAIC scores for each population separately with the polarity $AIC_x -$
219 AIC_2 , where AIC_x is the AIC score for model x and AIC_2 is the AIC score for the two-locus,
220 unlinked model. With this polarity, $\Delta AIC > 0$ indicates better fit of the unlinked two-locus
221 model relative to the alternative model. To estimate overall model fit, we summed ΔAIC
222 scores across populations. This operation is mathematically identical to computing ΔAIC
223 from the overall log-probability of the complete data vector. However, by decomposing the
224 overall ΔAIC into population-specific scores, we are able to visualize the extent to which
225 support for different models varies among populations in addition to presenting estimates of
226 "global" model fit.

227 *Power analysis and simulations*

228 We conducted parametric simulations under the fitted one- and two-locus models to
229 test (i) whether our approach has sufficient power to distinguish between the candidate
230 models given the sample sizes and phenotype distributions for each population, and (ii) the

231 overall goodness of fit of the simple models. Using the maximum likelihood estimates of
232 allele frequencies for each population under the one and two-locus unlinked models, we
233 simulated pseudo-populations of phenotypes assuming Hardy-Weinberg equilibrium. Each
234 simulated population was constrained to have the same number of individuals as the true
235 study population. For the i 'th population, a single instance of the simulation under the one-
236 locus model is as follows. Given maximum likelihood allele frequencies r_i , b_i , and n_i , we first
237 computed the equilibrium distribution of phenotypes under Hardy-Weinberg equilibrium
238 (e.g., expected "red striped" frequency = $r_i^2 + 2r_in_i$). We then sampled N_i phenotypes from
239 this distribution, where N_i is the number of individuals in the observed data for the i 'th
240 population.

241 We fitted one- and two-locus models to each such simulated dataset, to assess our
242 power to infer each scenario given a particular (known) model of inheritance. We graphically
243 compared distributions of phenotypes from populations simulated under each model to the
244 observed distribution as an initial test for model adequacy. We then computed the difference
245 in AIC scores (ΔAIC) for each population under the two models, which we always computed
246 with the polarity described above ($\text{AIC}_{\text{one-locus}} - \text{AIC}_{\text{two-locus}}$). Thus, under a true (generating)
247 one-locus model, we expect ΔAIC to be negative, as the one-locus model should have a lower
248 (better) AIC score. Conversely, under true (generating) two-locus model, we expect ΔAIC to
249 be positive. We performed 1000 simulations under both one- and two-locus models per
250 population. Finally, we assessed overall goodness-of-fit by comparing the observed ΔAIC
251 value (summed across all populations) to the simulated distributions of ΔAIC under perfect
252 one- or two-locus inheritance.

253

254 **Results**

255 *Sex linkage*

256 We found no evidence for significant sex linkage of ground snake coloration either in
257 the overall dataset ($\chi^2 = 6.26, P = 0.10$) or within any of the seven populations with large
258 enough sample sizes to test ($\chi^2 = 0-3.35, P = 0.34-1.0$), suggesting that coloration is an
259 autosomal trait.

260 *Spatial and temporal autocorrelation*

261 While we did find evidence of spatial autocorrelation among populations when
262 analyzing the frequency of morphs across all populations together (Mantel statistic $r = 0.472,$
263 $P = 0.001$), this effect was generally driven by low-sample size populations in close
264 proximity ($< 100\text{km}$) across the Great Plains and an interaction among populations across a
265 known taxonomic break (Western vs. Great Plains; Fig. 2; Table S1). We found that spatial
266 autocorrelation was weaker or absent when morph presence, which is perhaps a more robust
267 metric of polymorphism, was used instead of morph frequency ($r = 0.062-0.168, P = 0.017-$
268 0.346 ; Fig. 2). Across the Western clade populations, we found no evidence of spatial
269 autocorrelation in any phenotypic metric or distance class ($r = 0.117-0.190, P = 0.128-0.346$).
270 Overall, spatial autocorrelation was also reduced or eliminated when populations were
271 analyzed under the more stringent sampling criterion of 20 individuals per population
272 (compare Fig. 2a to 2b), although this reduced the dataset from 40 to 21 total populations. We
273 found no effect of temporal autocorrelation, either when analyzed separately ($r = -0.074-$
274 $0.243, P = 0.089-0.928$) or in a partial Mantel test simultaneously with the geographic
275 distance matrix (no change to significance class when compared to the pure spatial model in
276 any case).

277 *Model comparison*

278 We found strong support across populations for a multi-locus model over a single-
279 locus model, with an overall $\Delta\text{AIC} = 154.38$ in support of the two-locus model (Fig. 3; Table
280 S2). Twelve of these populations had AIC differences greater than +2 units, while no

281 population had significant support for the one-locus model (≤ -2 units; Fig. 3a). We found
282 that these differences in model support were not biased by levels of polymorphism ($F_{1,38} =$
283 1.53, $P = 0.223$; Fig. 3b) or sample size ($F_{1,38} = 1.69$, $P = 0.202$; Fig. 3c). Although we
284 found many populations with ΔAIC scores at or near 0 (support for neither model, $N = 20$),
285 the majority of these were populations from the Great Plains clade with a high frequency of
286 the uniform morph, usually in close geographic proximity to each other (*e.g.*, those
287 populations with statistically detectable spatial autocorrelation; Fig. 3a; Table S1). Four of
288 the 5 populations with the greatest ΔAIC score, which accounted for two thirds of the total
289 ΔAIC sum, were from the Western clade with no spatial dependency of phenotype.

290 We found no statistical evidence for strong linkage disequilibrium between the red
291 and black loci, with the unlinked two-locus model supported over both a) the linkage model
292 with D as a free parameter ($\Delta AIC = 29.52$ favoring the unlinked model), and b) the strong
293 linkage model with D fixed at the theoretical D_{\max} for each population ($\Delta AIC = 230.71$
294 favoring the unlinked model). These results for the strong linkage model were quite striking,
295 as the fit of this model was even worse than the fit of the one-locus model. Because the
296 number of parameters in the two-locus unlinked model and the strong-linkage model are
297 identical, this result is not merely driven by a difference in the number of parameters.
298 Additionally, these results do not depend on the precise relative D value used to define strong
299 linkage: even when we reduce relative D to 0.8, the unlinked model fits much better ($\Delta AIC =$
300 33.9). Although two populations had significant support for the linkage models when
301 analyzed independently (Carter Co., OK and Cowley Co., KS; Table S2), the low number of
302 mimetic individuals (3 and 2, respectively) driving this result suggests that this outcome more
303 likely results from violations of Hardy-Weinberg assumptions or population/morph
304 classification error than from true linkage.

305 Our power simulations (Fig. 4) indicate that we had high discrimination power among

306 the one- and two-locus models, even with low sample sizes. In populations with few uniform
307 morphs, we found that even low sample sizes (*e.g.*, $N = 10$) yielded substantially different
308 distributions of predicted numbers of mimetic individuals under the two models; these
309 distributions became even more distinct with greater sample size (Fig. 4a). In populations
310 with mostly uniform morphs, we found that increasing sample size had no effect on
311 distinguishing among models due to low information content (Fig. 4a). For the true sample
312 sizes in the observed data, we found that this effect of information content held across all
313 morphs, with observed numbers of the three non-uniform morphs supporting the two-locus
314 model for populations with high information content, while the models are indistinguishable
315 for the populations with low informativeness (Fig. 4b). When all populations are simulated
316 under one- vs. two-locus models, we found that support for the two models are easily
317 distinguishable (note non-overlapping distributions in Fig. 4c). Thus, our results cannot be
318 explained by an asymmetry in power to distinguish between one- and two-locus models.
319 Finally, the observed ΔAIC value across all populations is close to the distribution of
320 simulated values under a two-locus model and very different from the ΔAIC distribution
321 simulated under a one-locus model. The correspondence between the two-locus and observed
322 values is especially striking given the numerous ways that real populations can deviate from
323 the strict assumptions of Hardy-Weinberg equilibrium present in the simulation model.

324

325 **Discussion**

326 Here we have provided evidence that pigmentation genes for the mimicry of coral
327 snake coloration are controlled by separate loci and assort in an unlinked fashion in natural
328 populations of mimics. The support for a multi-locus system is unsurprising given what was
329 already known or suspected about pigmentation in snakes, but the evidence against strong
330 linkage between loci in a Batesian mimic is an exciting and unexpected result given the

331 supergene linkage repeatedly found in butterfly mimicry (Joron et al. 2006; Joron et al. 2011;
332 Kunte et al. 2014).

333 An important question that follows from our study is how generalized a lack of
334 linkage between red and black coloration may be across coral snake mimics, especially in
335 species that are not polymorphic. It is possible that *Sonora* represents an atypical loss of
336 linkage, perhaps as part of a northward expansion beyond the range of model species after the
337 last glacial maximum (Westphal et al. 2011), while linkage has been maintained across most
338 other mimetic species. However, many populations of *S. semiannulata* remain sympatric with
339 coral snakes (Cox and Davis Rabosky 2013), including as far south as the Mexican state of
340 Jalisco (*e.g.*, MZFC-17246). Additionally, the frequency and quality of color polymorphism
341 across both coral snakes and their mimics suggests that polymorphism is so common (Davis
342 Rabosky et al. in review) and repeatable (always the same general set of color morphs) that
343 *Sonora* likely represents a common condition in the evolutionary dynamics of coral snake
344 mimicry.

345 There are two competing explanations for this lack of genetic linkage that require
346 further testing. The first is that it is possible that the increased toxicity to the predator of
347 lethal coral snakes relative to merely noxious butterflies may lead to wholly different
348 dynamics and fitness costs in snakes during the evolution of mimicry from a cryptic ancestor
349 (Pough 1988). In this case, it may be useful to theoretically assess toxicity thresholds in
350 model species that are sufficient to prevent locus linkage in the mimics, perhaps akin to the
351 approach taken by Turner (Turner et al. 1984) or palatability, abundance, and fitness.
352 However, a second explanation suggests that coral snake mimicry may be more Müllerian
353 than commonly described (Greene and McDiarmid 1981). Coral snake mimicry has
354 traditionally been considered Batesian because there are no New World Colubrid snakes with
355 the advanced venom delivery system found in Elapids (front fangs, muscular control of

356 venom glands, complex venom cocktails with high LD₅₀ values, etc.) and no human or avian
357 deaths have ever been reported from a New World Colubrid bite (Weinstein et al. 2011).
358 However, many coral snake mimics, including *Sonora semiannulata*, have enlarged, grooved
359 rear teeth in association with a Duvernoy's gland and some level of toxicity to their prey
360 (Greene and McDiarmid 2005). The success of these modifications for predator defense
361 rather than prey acquisition, and therefore the nature and consequences of the boundary
362 between Batesian and Müllerian mimicry in snakes, is presumed to be inconsequential but
363 remains untested.

364 In either case, the lack of strong linkage between the two color components in coral
365 snake mimicry has major implications for the evolution of the mimetic signal over time. First,
366 because simple recombination is all that is needed for snake coloration to drastically change,
367 both the buildup and breakdown of the mimetic signal is likely to occur a) in discrete steps,
368 and b) quite quickly. Two unexplained observations about the relative rates of color evolution
369 among mimicry systems that may be impacted by genetic linkage is that the rates recovered
370 across phylogenies of snakes (Davis Rabosky et al. in review) are several orders of
371 magnitude faster than rates recovered in invertebrates (Kunte 2009; Oliver and Prudic 2010;
372 Penney et al. 2012) and that reversals back to the cryptic state are much more common in
373 snakes. Intriguingly, rates of color evolution across the genus *Heliconius*, which contains
374 mostly Müllerian mimics with unlinked coloration components (Kronforst and Papa 2015),
375 have been qualitatively inferred to be quite high (Kozak et al. 2015) and much more similar
376 to those recovered for snakes. Thus, coral snake mimicry may emerge as a surprising
377 demonstration of the greater importance of the genetic architecture behind the mimetic signal
378 than the classification of a system as Müllerian or Batesian in predicting the
379 macroevolutionary dynamics of mimetic signals.

380

381 **Acknowledgements**

382 We thank the following museums and their curatorial staff for access to specimens: Arizona
383 State University, California Academy of Sciences, Museum of Southwestern Biology at the
384 University of New Mexico, Museum of Vertebrate Zoology at the University of California,
385 New Mexico State University, Sam Noble Museum at the University of Oklahoma, San
386 Diego Natural History Museum, Sternberg Museum of Natural History at Fort Hayes State
387 University, University of Arizona, University of Kansas, University of Texas, University of
388 Texas at Arlington Amphibian and Reptile Diversity Research Center, and University of
389 Texas at El Paso. We thank two anonymous reviewers and M. Alfaro for helpful comments
390 on this manuscript, and Yann Surget-Groba for help sampling museum specimens. This work
391 was supported by a National Science Foundation Postdoctoral Fellowship in Biology (DBI-
392 0906046) to ARDR and by the University of Michigan. The authors declare no conflicts of
393 interest.

Literature Cited

- Bagnara, J. T. 1983. Developmental aspects of vertebrate chromatophores. *American Zoologist* 23:465-478.
- Bechtel, H. B. 1978. Color and pattern in snakes (Reptilia, Serpentes). *Journal of Herpetology* 12:521-532.
- Bechtel, H. B. and E. Bechtel. 1962. Heredity of albinism in the corn snake, *Elaphe guttata guttata*, demonstrated in captive breedings. *Copeia* 2:436-437.
- Bechtel, H. B. and E. Bechtel. 1978. Heredity of pattern mutation in the corn snake, *Elaphe g. guttata*, demonstrated in captive breedings. *Copeia* 4:719-721.
- Brodie, E. D., III and E. D. Brodie, Jr. 2004. Venomous snake mimicry. Pp. 617-633 in J. A. Campbell, and W. W. Lamar, eds. *Venomous reptiles of the Western Hemisphere*. Cornell University Press.
- Campbell, J. A. and W. W. Lamar. 2004. *The Venomous Reptiles of the Western Hemisphere*. Cornell University Press, Ithaca, NY.

- Charlesworth, D. 2016. The status of supergenes in the 21st century: recombination suppression in Batesian mimicry and sex chromosomes and other complex adaptations. *Evolutionary Applications* 9:74-90.
- Charlesworth, D. and B. Charlesworth. 1975. Theoretical genetics of Batesian mimicry II. Evolution of supergenes. *Journal of Theoretical Biology* 55:305-324.
- Charlesworth, D. and B. Charlesworth. 2011. Mimicry: The hunting of the supergene. *Current Biology* 21:R846-R848.
- Cox, C. L. and A. R. Davis Rabosky. 2013. Spatial and temporal drivers of phenotypic diversity in polymorphic snakes. *The American Naturalist* 182:E40-E57.
- Cox, C. L., A. R. Davis Rabosky, and P. T. Chippindale. 2013. Sequence variation in the *Mclr* gene for a group of polymorphic snakes. *Gene* 513:282-286.
- Cox, C. L., A. R. Davis Rabosky, J. Reyes-Velasco, P. Ponce-Campos, E. N. Smith, O. Flores-Vilella, and J. A. Campbell. 2012. Molecular systematics of the genus *Sonora* (Squamata: Colubridae) in central and western Mexico. *Systematics and Biodiversity*.
- Davis Rabosky, A. R., C. L. Cox, D. L. Rabosky, P. Title, I. A. Holmes, A. Feldman, and J. A. McGuire. in review. Coral snakes predict the evolution of mimicry across New World snakes. *Nature Communications*.
- Franks, D. W. and T. N. Sherratt. 2007. The evolution of multicomponent mimicry. *J Theor Biol* 244:631-639.
- Gamberale- Stille, G., A. C. Balogh, B. S. Tullberg, and O. Leimar. 2012. Feature saltation and the evolution of mimicry. *Evolution* 66:807-817.
- Greene, H. and R. McDiarmid. 2005. Wallace and Savage: Heroes, theories, and venomous snake mimicry. Pp. 190-208. *Ecology and Evolution in the Tropics: A Herpetological Perspective*. University of Chicago Press.
- Greene, H. W. and R. W. McDiarmid. 1981. Coral snake mimicry: Does it occur? *Science* 213:1207-1212.
- Joron, M., L. Frezal, R. T. Jones, N. L. Chamberlain, S. F. Lee, C. R. Haag, A. Whibley, M. Becuwe, S. W. Baxter, L. Ferguson, P. A. Wilkinson, C. Salazar, C. Davidson, R. Clark, M. A. Quail, H. Beasley, R. Glithero, C. Lloyd, S. Sims, M. C. Jones, J. Rogers, C. D. Jiggins, and R. H. ffrench-Constant. 2011. Chromosomal rearrangements maintain a polymorphic supergene controlling butterfly mimicry. *Nature* 477:203-206.
- Joron, M. and J. L. Mallet. 1998. Diversity in mimicry: paradox or paradigm? *Trends in Ecology & Evolution* 13:461-466.
- Joron, M., R. Papa, M. Beltrán, N. Chamberlain, J. Mavárez, S. Baxter, M. Abanto, E. Bermingham, S. J. Humphray, and J. Rogers. 2006. A conserved supergene locus controls colour pattern diversity in *Heliconius* butterflies. *PLoS Biology* 4:e303.
- Kikuchi, D. W. and D. W. Pfennig. 2012. A Batesian mimic and its model share color production mechanisms. *Current Zoology* 58.

- Kikuchi, D. W., B. M. Seymoure, and D. W. Pfennig. 2014. Mimicry's palette: widespread use of conserved pigments in the aposematic signals of snakes. *Evolution & Development* 16:61-67.
- Kozak, K. M., N. Wahlberg, A. F. Neild, K. K. Dasmahapatra, J. Mallet, and C. D. Jiggins. 2015. Multilocus species trees show the recent adaptive radiation of the mimetic *Heliconius* butterflies. *Systematic Biology* 64:505-524.
- Kronforst, M. R. and R. Papa. 2015. The functional basis of wing patterning in *Heliconius* butterflies: The molecules behind mimicry. *Genetics* 200:1-19.
- Kunte, K., W. Zhang, A. Tenger-Trolander, D. H. Palmer, A. Martin, R. D. Reed, S. P. Mullen, and M. R. Kronforst. 2014. *doublesex* is a mimicry supergene. *Nature* 507:229-232.
- Kuriyama, T., H. Misawa, K. Miyaji, M. Sugimoto, and M. Hasegawa. 2013. Pigment cell mechanisms underlying dorsal color-pattern polymorphism in the Japanese four-lined snake. *Journal of Morphology* 274:1353-1364.
- Leimar, O., B. S. Tullberg, and J. Mallet. 2012. Mimicry, saltational evolution, and the crossing of fitness valleys. *The Adaptive Landscape in Evolutionary Biology*. Oxford University Press, Oxford, UK:259-270.
- Mallet, J. and M. Joron. 1999. Evolution of diversity in warning color and mimicry: polymorphisms, shifting balance, and speciation. *Annual Review of Ecology and Systematics* 30:201-233.
- Mappes, J. and R. V. Alatalo. 1997. Batesian mimicry and signal accuracy. *Evolution* 51:2048-2051.
- Martin, A., R. Papa, N. J. Nadeau, R. I. Hill, B. A. Counterman, G. Halder, C. D. Jiggins, M. R. Kronforst, A. D. Long, W. O. McMillan, and R. D. Reed. 2012. Diversification of complex butterfly wing patterns by repeated regulatory evolution of a *Wnt* ligand. *Proceedings of the National Academy of Sciences* 109:12632-12637.
- Nijhout, H. F. 2003. Polymorphic mimicry in *Papilio dardanus*: mosaic dominance, big effects, and origins. *Evolution and Development* 5:579-592.
- Pough, F. H. 1988. Mimicry of vertebrates: Are the rules different? *The American Naturalist* 131:S67-S102.
- Reed, R. D., R. Papa, A. Martin, H. M. Hines, B. A. Counterman, C. Pardo-Diaz, C. D. Jiggins, N. L. Chamberlain, M. R. Kronforst, R. Chen, G. Halder, H. F. Nijhout, and W. O. McMillan. 2011. *optix* drives the repeated convergent evolution of butterfly wing pattern mimicry. *Science* 333:1137-1141.
- Rosenblum, E. B. 2006. Convergent evolution and divergent selection: Lizards at the White Sands ecotone. *The American Naturalist* 167:1-15.
- Rosenblum, E. B., H. Rompler, T. Schoneberg, and H. E. Hoekstra. 2010. Molecular and functional basis of phenotypic convergence in white lizards at White Sands. *Proceedings of the National Academy of Sciences of the United States of America* 107:2113-2117.
- Savage, J. S. and J. B. Slowinski. 1992. The colouration of the venomous coral snakes (family Elapidae) and their mimics (families Aniliidae and Colubridae). *Biological Journal of the Linnean Society* 45:235-254.

- Turner, J. R. G. 1987. The evolutionary dynamics of Batesian and Muellierian mimicry: similarities and differences. *Ecological Entomology* 12:81-95.
- Turner, J. R. G., E. P. Kearney, and L. S. Exton. 1984. Mimicry and the Monte Carlo predator: the palatability spectrum and the origins of mimicry. *Biological Journal of the Linnean Society* 23:247-268.
- U.S. Census Bureau. 2011. USA counties data file downloads. Spreadsheet LND01.xls.
- Weinstein, S. A., D. A. Warrell, J. White, and D. E. Keyler. 2011. "Venomous" Bites from Non-Venomous Snakes: A Critical Analysis of Risk and Management of "Colubrid" Snake Bites. Elsevier.
- Westphal, M. F., J. L. Massie, J. M. Bronkema, B. E. Smith, and T. J. Morgan. 2011. Heritable variation in garter snake color patterns in postglacial populations. *PLoS ONE* 6:e24199-e24199.
- Westphal, M. F. and T. J. Morgan. 2010. Quantitative genetics of pigmentation development in 2 populations of the Common Garter Snake, *Thamnophis sirtalis*. *Journal of Heredity* 101:573-580.
- Wright, S. 1943. An analysis of local variability of flower color in *Linanthus parryae*. *Genetics* 28:139-156.

Author Manuscript

Figure Legends

Figure 1. Three dimensional bar plots of counts for four sympatric color morphs by population across the continental United States (a) mimetic, (b) banded, (c) striped, (d) uniform. All bars are plotted on the same scale, and the highest bar (Maricopa Co., AZ, striped morph) represents 150 individuals.

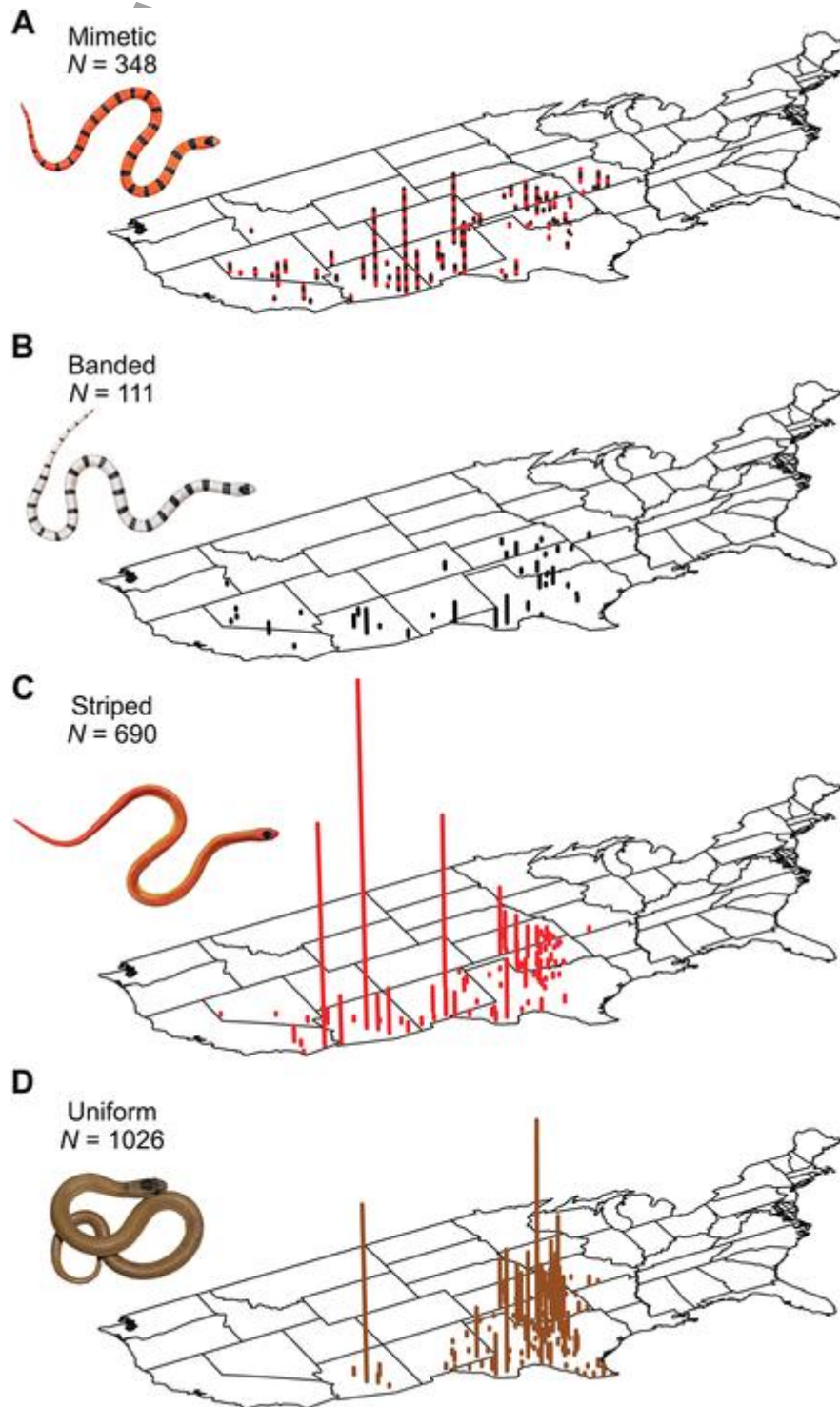


Figure 2. Mantel correlograms between phenotypic and geographic distance by class using populations with (a) at least $N = 12$ and (b) at least $N = 20$ individuals sampled within a 20-year time window. Filled symbols indicate distance classes with significant correlation. Y-axis ranges are standardized to aid comparison among plots.

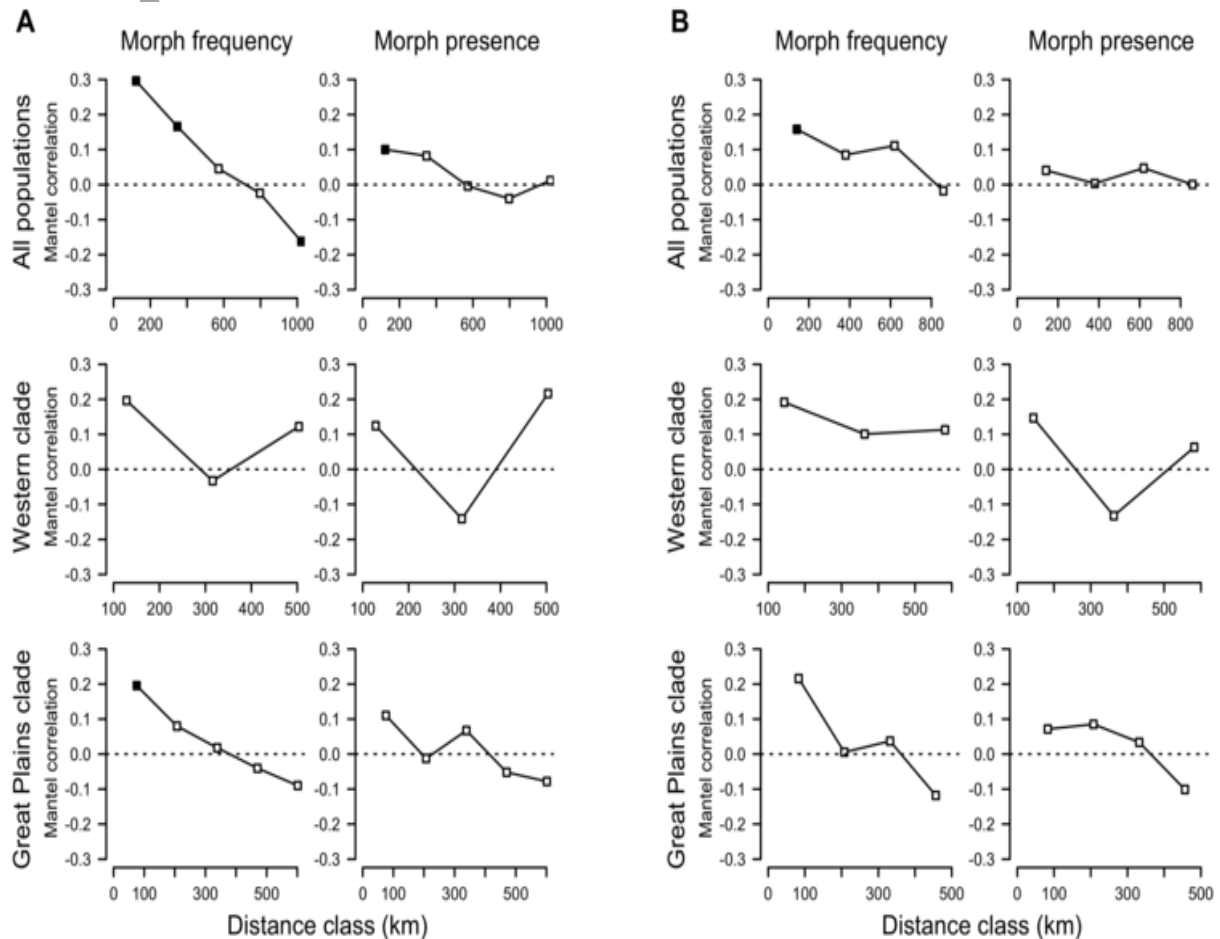


Figure 3. (a) Comparisons of model fit ($N = 40$ populations) show strong overall support for the two-locus model (sum of $\Delta AIC = 154.36$; note that 4 of the 5 highest scoring populations are from the Western clade). No populations show significant support for the one-locus model. Dashed reference line for equivocal model support is given at 0. (b) Model fit shows no relationship with level of polymorphism ($F_{1,38} = 1.53$, $P = 0.223$). (c) There is no correlation between between the number of snakes collected within a population and the number of morphs detected ($F_{1,38} = 1.69$, $P = 0.202$). Asterisked P -values are from linear models without the respective outlier values. Note the broken axis in each panel to allow the display of outlying values.

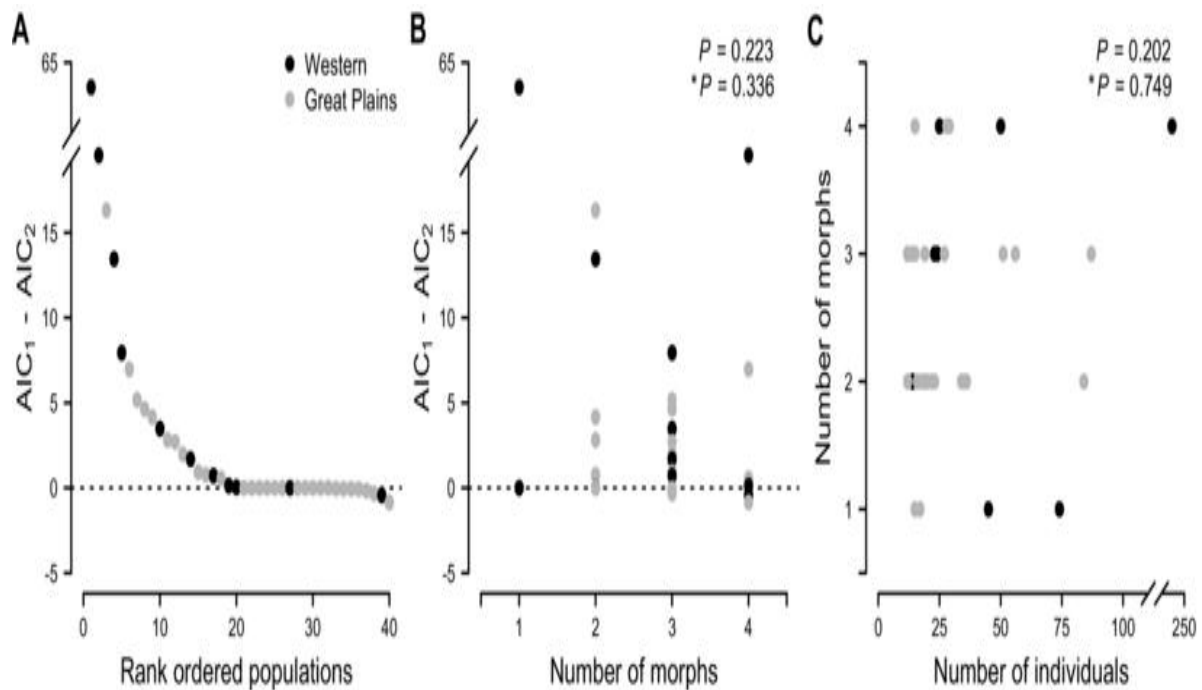
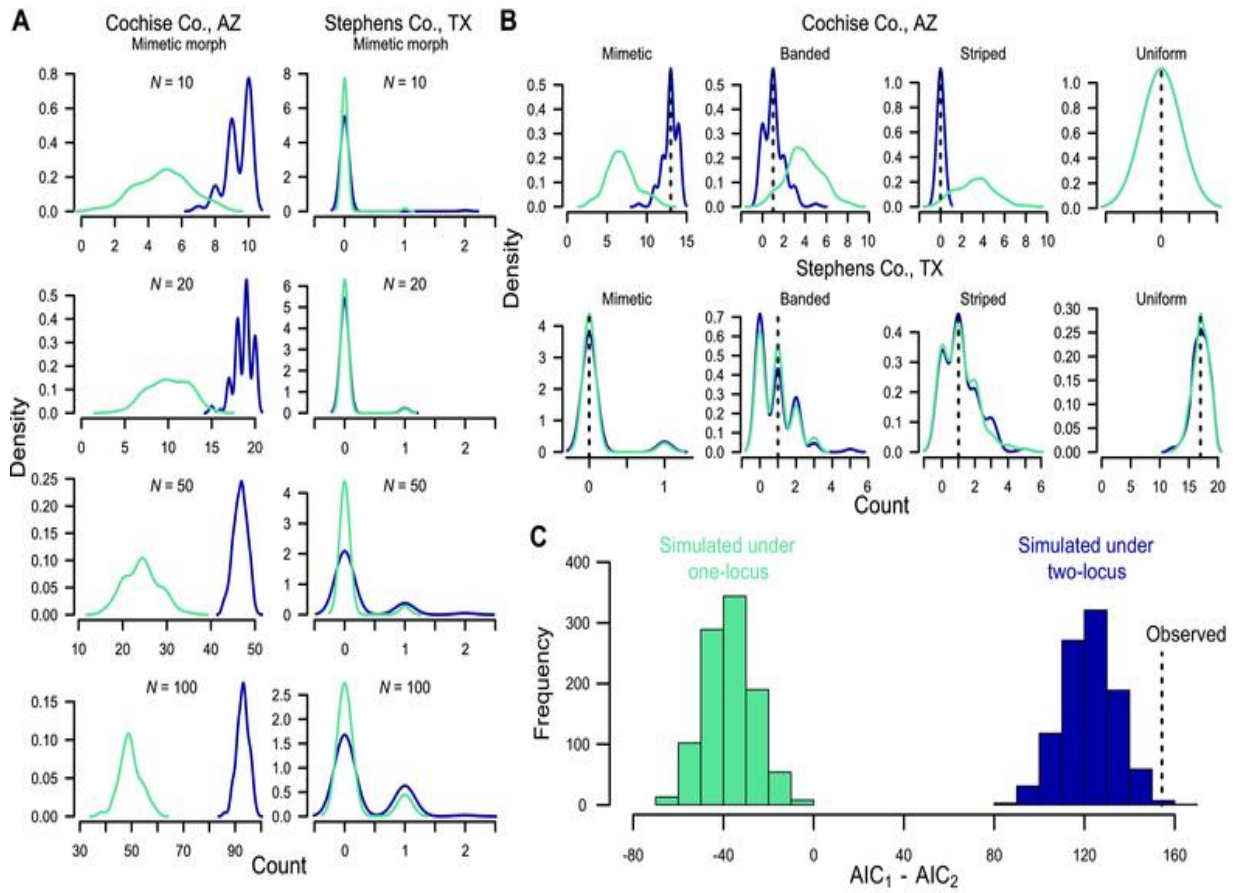


Figure 4. Simulated power analyses, with one-locus model predictions in light blue and two-locus predictions in dark blue. (a) Kernel density plots of populations with mostly non-uniform morphs (e.g., Cochise Co., AZ) show substantially different distributions of predicted numbers of mimetic individuals under the two models at all sample sizes, while increasing sample size has no effect on distinguishing among models in populations with high frequencies of the uniform morph (e.g., Stephens Co., TX) due to low information content. (b) For the true sample sizes in the observed data for the same two populations ($N = 14$ for Cochise Co. and $N = 19$ for Stephens Co.), the observed numbers of each morph (dashed lines) support the two-locus model for the population with high information content, while the models are indistinguishable for the population with low informativeness. (c) When all populations are simulated under one- vs. two-locus models ($N = 1000$ iterations), support for the two models are easily distinguishable (note non-overlapping distributions) and our observed ΔAIC value (dashed line) fits a two-locus model much better than a one-locus model.



Author M